An Optimized Decentralized Power Sharing Strategy for Wind Farm De-Loading

Xinkai Fan, *Student Member, IEEE*, Emanuele Crisostomi, *Senior Member, IEEE,* Dimitri Thomopulos, Baohui Zhang, *Fellow, IEEE,* Robert Shorten, *Senior Member, IEEE,* and Songhao Yang, *Member, IEEE*

***Abstract*—Many centralized and distributed power sharing algorithms have been proposed in the literature for de-loading operations in wind farms with variable speed wind turbines. Typically, in these strategies, two-way communications are required between the control center and the single turbines, or among the turbines. This paper solves the same problem in a truly decentralized fashion, which only requires a greatly reduced amount of one-way communications, without exchanging information among the turbines, and shows that an optimal solution can be obtained to minimize utility functions of interest of single wind turbines. In particular, we consider utility functions that take into account mechanical fluctuations and rotor over-speeds during transient, while balancing the utilization of wind turbines at steady-state operations. This is achieved by adopting the so-called Additive Increase Multiplicative Decrease (AIMD) algorithms, which are frequently used in communication applications, for solving the power sharing problem in a decentralized fashion. Extensive simulations under different working conditions, on wind farms consisting of wind turbines of different mechanical characteristics, are provided to illustrate the potential and the efficiency of the proposed methodology.**

***Index Terms*—AIMD, Decentralized Control, Power Sharing, Wind Energy**

I. Introduction

A. Motivation

Energy generation from renewable sources is definitely helping to achieve worldwide green targets, but it is undoubtedly raising concerns of grid operators, who need to keep matching demand and supply in a more uncertain scenario. Therefore, in the context of wind generation, there is an increasing interest in Variable Speed Wind Turbines (VSWTs), as their flexibility may be used to mitigate the otherwise uncertain, and not accurately predictable, power generation [1]. In fact, the power electronic converters of VSWTs allow them to track maximum power over a wide range of wind speeds [2]. In addition, VSWTs can be also operated in a de-loaded regime, which consists of extracting less power than the maximum available one [3]–[6]. For instance, the purpose of de-loading could be meeting the transmission capacity or load limitation [3], or ensuring transient stability [4], or in general obtaining more flexibility in regulating the power generation of a wind farm for frequency support [5] or power oscillation damping [6].

In this work, X. Fan was partially supported by the key project of National Natural Science Fund (U1766209) and China Scholarship Council. Also, E. Crisostomi, D. Thomopulos, and X. Fan were partially supported by MIUR under PRIN 2017 grant "Advanced Network Control of Future Smart Grids" and partially supported by the European Union's Horizon 2020 research and innovation programme under grant agreement No 863922.

X. Fan, B. Zhang, and S. Yang are with the State Key Laboratory of Electrical Insulation and Power Equipment, Xi'an Jiaotong University, Xi'an, China (e-mail: fanxinkai@stu.xjtu.edu.cn, {bhzhang, songhaoyang}@xjtu.edu.cn).

E. Crisostomi and D. Thomopulos are with the Department of Energy, Systems, Territory and Constructions Engineering (DESTEC), University of Pisa, Pisa, Italy (e-mail: {emanuele.crisostomi, dimitri.thomopulos}@unipi.it).

X. Fan is also with the DESTEC, University of Pisa, Pisa, Italy.

R. Shorten is with the Dyson School of Design Engineering Imperial College London, London, UK (e-mail: r.shorten@imperial.ac.uk).

B. State of the art

De-loading is, therefore, a crucial activity to be decided by the grid operator managing the wind farms (WF). Typically, the amount of power to share among the different Wind Turbines (WTs) is determined by the WF operator, but different power sharing strategies can be chosen as [7]–[17]. Among the strategies present in the literature, the first distinction that can be noticed is the level of centralization. There are indeed centralized or distributed approaches. Considering centralized solutions, the simplest strategy is to equally share the power references among the WTs [7]. A more sophisticated version was proposed in [8] where a centralized optimizing power sharing method was used to seek the minimum of active power losses in a wind farm. In [9], an efficient and fair load-sharing strategy was proposed, which calculated the references proportionally to the available active powers. In [10], a wind farm controller design was proposed to minimize the wind turbine mechanical stress loads. In [11], the power reference of each WT was computed to maximize the rotor kinetic energy. Similarly in [12], the kinetic energy was maximized while further considering the wake interactions in the wind farm. In [13], a centralized optimal power control strategy was proposed to minimize the wind tower torque and to make each turbine work close to its optimal working point.

One of the major disadvantages of applying centralized methodologies is certainly the high and frequent flow of bi-directional information between the WTs and the WF control center. This obviously entails a high overall communication burden, as well as it creates possible issues in terms of communication delays or noise, and in general produces a less robust solution. For these reasons, recent works have been more oriented towards distributed approaches for power sharing [14]–[17]. In [14], the wind turbine loads were minimized through a distributed model predictive control of a WF. In [15], a fairly share of load was obtained by adopting a Leader-Follower consensus protocol, through a distributed torque control method. In [16], a game theory distributed approach was proposed, where the rotational kinetic energy stored in the WTs was maximized. Finally, in [17], a sparse communication network was proposed to implement a coordinated power control of a WF, to reduce the fatigue loads of WTs. It is important to note that such solutions are not fully distributed in reality, as a central control unit is required anyway to communicate the power reference (i.e., de-loading signal) to the wind turbines. Nevertheless, the computational burden of the central unit is significantly reduced with respect to a centralized implementation [14].

C. Contributions

Another interesting classification among the aforementioned references may be performed on the basis of how the optimal power sharing decision is taken. In particular, it can be noticed that some of the references focus on optimizing a transient objective, i.e., related to physical quantities like the thrust or the torque. Other references focus on steady-state objectives, which usually involve quantities like the stored kinetic energy, power losses, or deviations from maximum-power-point. In this paper, we take into account both the transient and the steady-state aspects, by considering a utility function of interest that contains both components. In addition, we take into special account the transient rotor over-speed, which has been neglected by most references, while actually it is a relevant problem as it may lead to the WT protection trippings and ultimately to unexpected power drops in a WF. Also, we consider aging aspects in the steady-state component of our utility function, which is another aspect that is usually neglected in the literature.

In addition to choosing a different utility function, we also propose an alternative decentralized solution of the power sharing optimization problem. In fact, while distributed methodologies (e.g., papers [14]–[17]) successfully manage to split the original centralized control problem into a number of smaller separate control problems, still significant two-way communications are required between the aggregator (i.e., the WF control center) and the single WTs, or, in cases of fully distributed solutions, among the WTs. On the other hand, in this paper, we present a truly decentralized solution for the power sharing problem, which optimally manages to solve the de-loading problem with a greatly reduced amount of communication and, in particular, without requiring to exchange information among the WTs. For this purpose, we borrow Additive Increase Multiplicative Decrease (AIMD) methodologies, which have been widely used to solve internet congestion problems [18], and in general many optimal resource allocation problems [19]. Such methodologies only require non-frequent one-way notifications from the WF control center to automatically share the de-loading task as preferred. Besides, AIMD algorithms also bring benefits of so-called “Plug & Play” features, to automatically redistribute power generation among WTs when start/stop events occurs (e.g., start another WT from off-state, or a sudden stop of a WT in operation), without any difference with respect to the nominal operation.

Some preliminary results of a decentralized solution of the power sharing problem have been presented in [20]. In [20], the de-loading action had been implemented simply proportionally to the power that could be generated by each WT. Here, we show how the de-loading action can be implemented in order to minimize a utility function of interest that, as mentioned, involves transient and steady-state aspects. Accordingly, a different algorithm is required to solve the optimization problem in a decentralized fashion.

The rest of this paper is organized as follows: Section II illustrates the basic models of VSWTs and WFs which have been used in this paper. Section III briefly revises the state-space model of VSWTs, and then illustrates how the control problem is formulated and solved in an AIMD framework. Then, simulations results are described in Section IV, while Section V summarizes our findings and concludes the paper.

II. Model of a Wind Farm

A. Wind Turbine Characters and Control

Two types of VSWTs, Doubly-Fed Induction Generator (DFIG) and Permanent Magnet Synchronous Generator (PMSG), are popularly used in large-scale wind generation [2] nowadays. The converters in both two types of wind turbines have the ability to decouple the rotor speed from the output provided power, and to generate electricity with a constant frequency for different rotor speeds. In addition, both types of WTs have wind blade wheels with similar characteristics, and have the same pitch control mechanisms.

We now briefly recall the basic equations that describe the mechanical movement of WTs, following the work of [21]. When wind passes through the wind blades, some of its energy is converted into the mechanical power P_{wm} of the rotor, as:

$$P_{wm} = \frac{1}{2}\rho\pi R^2 v_w^3 C_p(\theta,\lambda) \tag{1}$$

where P_{wm} is the input mechanical power, C_p is the power coefficient, ρ is the air density, R is the turbine rotor radius, v_w is the effective wind speed, λ is the tip-speed ratio equal to $R\omega_r/v_w$, ω_r is the rotor speed, and θ is the pitch angle. When power losses and damping effects are neglected, the rotor speed ω_r is related to the electrical torque T_e and mechanical torque T_r as follows:

$$J_t\frac{\mathrm{d}\omega_r}{\mathrm{d}t} = T_r - T_e \tag{2}$$

where J_t is the inertia of the motion system, $T_r = P_{wm}/\omega_r$, $T_e = P_e/\omega_r$, and P_e is the electrical power. In consideration of the rapid converter response speed, the actual output electrical power P_e can be approximately replaced by the controller's reference electrical power P_{ref}. And the shaft torque T_s can be computed as:

$$T_s = \frac{J_g}{J_t}T_r + \frac{J_r}{J_t}T_e \tag{3}$$

where J_r and J_g are the impeller and generator inertia, respectively, and $J_t = J_r + J_g$.

Also, the other part of wind energy takes a thrust force F_t on the rotor plane, which is related to the thrust coefficient C_t:

$$F_t = \frac{1}{2}\rho\pi R^2 v_w^2 C_t(\theta,\lambda). \tag{4}$$

B. Wind Turbine Control

In principle, many different control strategies have been proposed to control wind turbines. However, three areas of operation are classically identified: 1) Maximum power point tracking (MPPT); 2) Constant rotor speed control; 3) Constant power control. And these functions are typically achieved by combining the pitch control of the WT with the converter's electromagnetic power control.

The block diagram summarizing a typical simplified pitch angle controller of VSWTs is shown in Fig. 1,

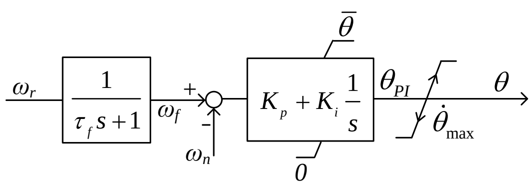

Fig. 1. Basic structure of pitch controller

where ω_f is the filtered rotor speed, ω_n is the rated rotor speed, $\bar{\theta}$ is the upper limit of the pitch angle, $\dot{\theta}_{max}$ is the limitation of the pitch regulation rate, τ_f is the time constant of the first-order filter, θ_{PI} is an intermediate quantity given by PI controller, and K_p and K_i are the control parameters of the PI pitch controller. The blocks contain the transfer functions of the different components, in the classic Laplace domain.

Coordinating this pitch controller with the converters' electromagnetic power control, the implementation of WT control in full-wind-range is that: Under low-wind-speed, the pitch angle is fixed to its initial value and the WT's rotor speed adjusts through the electromagnetic power control to achieve MPPT. Under high-wind-speed, the electromagnetic power control maintains its maximum, and the pitch angle control is activated to ensure generation at the maximum safe rotation.

By slightly modifying the above mentioned classical control, the WT level de-loading control process applied in this paper is briefly illustrated in Fig. 2. Roughly speaking, when the wind is low, the rotor speed is modified to follow the reference electrical power P_{ref}, while at higher wind speeds the pitch control is used to change the power curve. It may be interesting to notice that, at large wind speed conditions, if the electromagnetic power is rapidly reduced, then the input mechanical power does not change immediately due to the limitation of the pitch regulation rate and the rotor inertia. Thus, the unbalanced power accelerates the rotor during the transient. If the rotor speed exceeds its maximum value, then the speed protection is triggered for safety reasons and trips the wind generator. Therefore, both the magnitude and the rate of change of the de-loading control should be taken into consideration.

C. Wind Farm and its Control

A wind farm usually consists of tens to hundreds of WTs, and typically the coordination between WTs and the system operator is accomplished by using a centralized WF control system. The wind farm controller has the main objective of controlling the power production of the whole wind farm.

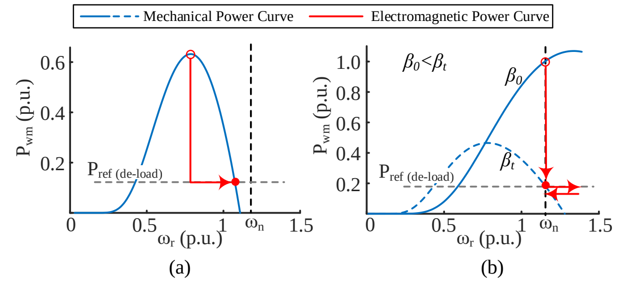

Fig. 2. Wind turbine under de-loading status (a) low wind speed, (b) high wind speed.

When the power system desires the WF to provide as much power as possible, the WF control center gives order to each WT to generate its maximum power. However, as previously mentioned, for the convenience of power system dispatching, a WF may actually have to follow a predefined output power curve. In this case, a traditional solution is using a centralized control unit, which typically has several inputs and outputs. For instance, the input signals may be system operator orders, measurements from the outgoing transmission lines, or information from WTs. Thus, a widely adopted centralized strategy is the so-called "fair" de-loading sharing [8], [13], [15], [20]. The basic idea is that if the WF has to decrease its power generation of a given percentage, then each WT should reduce its power generation by the same percentage. The power reference for each turbine is thus computed as

$$P_{ref(i)}(t) = \frac{\overline{P}_i(t)}{\sum_{i=1}^{n} \overline{P}_i(t)} P_{dem}(t) \tag{5}$$

where n is the number of WTs, $P_{ref(i)}(t)$ and $\overline{P}_i(t)$ are the reference power and the maximum power that could be generated by the i^{th} WT at a given time (i.e., with a given wind speed), and $P_{dem}(t)$ is the power demand for the whole WF. Hence, a centralized solution of problem (5) is that each individual WT sends information about its power capability to the WF controller. Then the WF controller sums all terms, calculates single reference powers, and dispatches back the power references to all WTs [9].

The "fair" strategy is simple and efficient, however it is not optimal in general. Some centralized optimization strategies considering kinetic energy stored in WT's rotor, torque, thrust, load and so on are presented in [7]–[13], but they are more complicated to implement, as they require a frequent exchange of information between the control center and the WTs, regarding wind speed, rotor speed, output power, or other measured mechanical variables. This obviously increases the computation and communication burdens, especially in large-scale WFs. For this reason, in the next section we describe our proposed truly decentralized solution for the power sharing problem, which optimally manages to solve the de-loading problem with a greatly reduced amount of communication.

III. Decentralized AIMD Control of the Wind Farm

A. Optimization Problem and Utility Function

The optimization problem consists of optimally allocating the power generation task, so that the overall generated power matches the power requested by the system operator, and each WT operates in a feasible range. Hence at each time step k, the power sharing optimization problem can be formulated as

$$\begin{aligned} &\min \sum_{i=1}^{n} f_i(P_{ref(i)}) \\ &s.t. \sum_{i=1}^{n} P_{ref(i)}(k) = P_{dem}(k) \\ &\underline{P}_i(k) \le P_{ref(i)}(k) \le \overline{P}_i(k) \quad \forall i = 1, ..., n, \end{aligned} \tag{6}$$

where $\underline{P}_i(k)$ and $\overline{P}_i(k)$ are the lower and upper bounds of the power that can be generated by the i^{th} WT at time step k, respectively, and n is as usual the number of WTs.

The optimal solution is then obtained by minimizing the cost function of interest. While many polices can be chosen for this purpose, here we consider three different aspects, as explained in detail in the following:

1) **Give priority to newer WTs**: This part prioritizes newer wind turbines to produce more power and undertake more dynamic stress. Typically, a large-scale wind farm is built in different stages, with different ages of possibly different WTs. With the aging of the WT, its reliability is gradually reduced, and the cost of operation and repairing is also gradually increased [22]. Generally speaking, a WT's aging rate is closely related to the generated output power, and to the hours of utilization t_u, which can be defined as:
$$t_u = \frac{\int_0^{t_{opr}} P_{wm}(t)\mathrm{d}t}{P_{rate}} \tag{7}$$
where the t_{opr} is the total running time of the WT from production till now, and P_{rate} is the rated power of the WT. The value of t_u can be easily obtained from WT historical data, and is an effective index to evaluate their age. While other indicators may be used as an alternative, the ultimate goal is to allow WFs to prioritize newer WTs with lower t_u and try to balance aging of WTs.
2) **Minimize the dynamic stress loads of the WT**, as in [10], [14], [17]: This part aggregates two kinds of dynamic stress loads on the wind turbine. The first part is the cycled thrust passed from the blade plane to the tower structure. Due to the elasticity of the WT structure, the thrust force F_t causes nodding of the tower, and an improper design of power sharing could amplify the tower oscillations and eventually lead to a break down of the WT. The second part is the torque T_s on the gearbox or shaft coupling. Since it is hard to accurately predict the wind speed, and the load sharing control may continuously modify the electromagnetic power, the oscillatory transient on the shaft could cause micro-cracks in the material. This can further lead to component failure, as for example a shaft fracture. Compared with static loads, the dynamic stress causing the structural damage of the wind turbine is considered as the most critical concern.
3) **Avoid over-speed problems during the transient**: The objective of this part is to avoid an unexpected transient over-speed wind turbine tripping during large and rapid power adjustments. As mentioned before, when the converters in VSWT instantly change the output electromagnetic power, the input mechanical power does not change instantaneously. Therefore, the unbalanced power will accelerate or decelerate the rotor, which may cause the rotor to exceed the speed limit during the transient. VSWTs are usually equipped with speed protection systems, which will trip the WT under such conditions. This situation should be prevented from occurring for the reasons that a) it is a huge impact on the WT itself; b) the WF instantly loses the over-speed WTs' power, and in turn the WF may fail to follow the desired power reference signal. Since the primary goal of the de-loading control is to ensure that the total output of the wind farm matches the system operator's required one, WTs should not be accidentally tripped, independently from their operational age.

Considering the three aspects mentioned above, our utility function for the i^{th} WT is computed as

$$\begin{aligned} f_i(P_{ref(i)}) =& Q_{F(i)} \frac{t_{u(i)}}{\hat{t}_u} (\frac{\mathrm{d}F_{t(i)}}{\mathrm{d}t})^2 + Q_{T(i)} \frac{t_{u(i)}}{\hat{t}_u} (T_{s(i)} - \hat{T}_{s(i)})^2 \\ &+ Q_{\omega(i)} (\Omega_i)^2 + Q_{P(i)} \frac{t_{u(i)}}{\hat{t}_u} P_{ref(i)}^2 \end{aligned} \tag{8}$$

where $Q_{F(i)}$, $Q_{T(i)}$, $Q_{\omega(i)}$ and $Q_{P(i)}$ are the weighting factors (which may be chosen to reflect the preferences of single WFs), $\hat{t}_u$ is the normalization coefficient of wind turbines' utilization hours, which is defined as the maximum $t_{u(i)}$ of WTs in the whole wind farm.

In the following, we explain in detail how the utility function aggregates the previously mentioned three different aspects. At steady-state, the first three terms are practically equal to zero and the last term takes a leading role, and is used to prioritize newer WTs. During the transient stage, the first two items can be used to minimize the dynamic stress loads of the WT, by reducing the oscillations of the thrust force F_t and torque T_s [10], [14], [17]. Finally, the third part is used to prevent over-speed problems from occurring, where Ω_i represents the over-speed influence and is given as

$$\Omega_i = \max\left[(\omega_{pre(i)} - \omega_{ub}), 0\right] \tag{9}$$

where ω_{ub} is the upper bound constant (for safety reasons) of the rotor speed, and $\omega_{pre(i)}$ is the maximum of the predicted value of the rotor speed for the next few seconds. The practical computation of the utility function, based on the states of the WTs, follows classic reference like [10], [14] and [17]. For convenience, we report such procedure in Appendix A.

Remark - choice of weighting factors: The weigthing factors $Q_{F(i)}$, $Q_{T(i)}$, $Q_{\omega(i)}$ and $Q_{P(i)}$ can be tuned by the operator of the WF, to prioritize one aspect over the others.

In our experience, over-speed is the most important issue and $Q_{\omega(i)}$ should have the highest value. Also, during the transient state of rapid power adjustment, we believe that reducing the fluctuation of thrust and torque is important and the optimized result should not be dominated by the steady-state power output, hence we make $Q_{F(i)}$ and $Q_{T(i)}$ higher than $Q_{P(i)}$. In addition, the selection of these weight coefficients is also related to the parameters of the WT. For example, a WT with a larger inertia requires a larger $Q_{\omega(i)}$ for proper rotor speed response. Our utility function allows different WFs' operators to choose different weigthing factors according to possible different priorities and WT parameters, and we recommend that it is better to optimize and determine the weight coefficient for a specific project through simulation and practical tests. Finally, we set ω_{ub} in (9) as 1.00 p.u. of the rated speed (which in turn is typically 1.2 p.u. of the synchronous speed [26], [27]). Accordingly, as soon as the speed exceeds the rated speed, the speed limit becomes effective.

B. AIMD Implementation

The problem of optimal allocation of a shared resource arises in many different scientific and engineering applications. The AIMD algorithm, which has been widely used in dealing with internet congestion, may be efficiently used to solve this problem. Assuming that n agents share the same resource, the basic rules underneath AIMD are [19]:

1) Each agent linearly increases its share of utilization of the resource when the total demand is less than the available capacity (Additive Increase, AI).
2) Each agent multiplicatively reduces its share of utilization of the resource when it is notified that the global capacity has been reached (Multiplicative Decrease, MD).

When the above principles are applied to the WF de-loading power sharing problem, the implementation is that each WT usually increases its power generation independently (AI), and if the total output of the WF is higher than power system operator's demand, then the control center broadcasts an MD bit flag to ask WTs to reduce their power generation (MD).

In addition, un-synchronized AIMD can be used to allocate the resource in an optimal fashion, here, to solve the optimization problem (6), by letting only a subset of the WTs to perform the MD step when a congestion event (i.e., the total output of the WF is higher than demand) occurs, while the others keep increasing their output power. In this way, it is possible to take into account the different needs of single WTs (i.e., their utility functions). In particular, each WT performs the multiplicative decrease with a locally computed probability [24]

$$\pi_i(P_{ref(i)}) = \Gamma \frac{f_i'(P_{ref(i)}(t))}{\hat{P}_{ref(i)}} \tag{10}$$

where $\hat{P}_{ref(i)}$ is the long-term average of the $P_{ref(i)}$, $f_i'(P_{ref(i)})$ denotes the derivative of the cost function, and Γ is a preset constant ensuring that $0 \leq \pi_i(P_{ref(i)}) \leq 1$ for $P_{ref(i)}, \forall i = 1, ..., n$. Equation (10) implies that each WT will react to a congestion event independently from the other WTs, with a customized probability $\pi_i(P_{ref(i)})$. The proposed algorithm, adapted for utility optimization purposes, is presented in Algorithm 1.

Algorithm 1. AIMD Utility Optimization

Input: $P_{ref(i0)}, \Gamma, t, \alpha, \beta, \overline{P}_i(t), \underline{P}_i(t)$
Output: $P_{ref(i)}$
$P_{ref(i)}(0) = P_{ref(i0)}$
repeat
  $t = t + 1$
  if $\sum_{i=1}^{n} P_{ref(i)}(t) > P_{dem}(t)$ &
    $\pi_i(P_{ref(i)}) > \text{rand}(1)$ **then**
    $P_{ref(i)}(t+1) = \max\left[\beta P_{ref(i)}(t), \underline{P}_i(t))\right]$
  else
    $P_{ref(i)}(t+1) = \min\left[P_{ref(i)}(t) + \alpha, \overline{P}_i(t)\right]$
  end if
until end of de-loading

If we assume that the optimization problem (6) is feasible (i.e., this can not be given for granted, as the system operator may request more power than the WTs may actually generate depending on wind conditions), and that de-loading occurs at a rather slow time scale (i.e., convergence to the required power reference signal occurs before a new power reference signal is requested by the system operator), then the convergence analysis described in [24, Section 4] can be used, and the AIMD algorithm 1 produces a long-term average that converges almost surely to the optimal solution of problem (6), see [24, Theorem 4.2].

In practical application, the only communication required to solve the optimization problem using Algorithm 1, is an MD signal that is broadcasted to all WTs by the WF operator, when P_{out} is greater than P_{dem}. Thus, in particular, single WTs receive the MD signal, but never send any information to neither other WTs, nor to the control center of the WF. However, they need sensors to measure the variables required to locally compute their own utility function.

In addition, the AIMD strategy does also provide the benefit that WTs can join and leave the de-loading task without any centralized supervision, thus giving rise to a wind generation system that is "plug & play" features, to automatically redistribute power generation among WTs when start/stop events occur (e.g., start another WT from off-state, or a sudden stop of a WT in operation), without any difference with respect to the nominal operation.

Remark - choice of parameters: The multiplicative parameter β must be positive and smaller than 1. Usually, it is chosen in the range [0.9, 1) to mitigate the impact of the multiplicative decrease step. On the other hand, there is not a "rule-of-thumb" choice for the positive parameter α, as it actually depends on the application of interest, and in the unit of measurement adopted in the equation (i.e., in our example α is directly added to the per unit power reference, and $\alpha \in [0.01, 0.025]$ has been tested to have good response characteristics). Finally, Γ is a constant required to map ratio (10) into a probability (i.e., between 0 and 1). Again, there is

TABLE I
ALGORITHM PARAMETERS

$Q_{F(i)}$	$Q_{\omega(i)}$	$Q_{P(i)}$	$Q_{T(i)}$	α	β	Γ
2	40	0.5	3 (DFIG), 1 (PMSG)	0.015	0.9	0.75

not a general rule to compute it (as it depends on the values that can be achieved by the derivatives of the utility functions, and thus, depends for instance on the choices of the other parameters Q as well). Here we consider a constant Γ, while in principle some more refined strategies have been proposed in the literature to iteratively estimate Γ in real-time (see for instance [19]).

IV. SIMULATION RESULTS

In this section, we provide the results of some simulations which we have performed to validate the proposed decentralized wind power sharing methodology. In particular, the first case study examines the performance in a de-loading situation, while the second case study emphasizes the "plug & play" capability of the proposed algorithm. Simulations were performed using the Matlab-Simulink environment. The WF contains 5 PMSG WTs (No. 1 to 5) and 5 DFIG WTs (No. 6 to 10), all of 5 MW of size. For the sake of convenience, we assume that all WTs have the same parameters but may have a different structure (given in Appendix B), and the aerodynamic characters C_t and C_p as from [21]. The control parameters and utilization hours for each WT are also given in Appendix B. Our choice of the de-loading factors is summarized in Table I. It should be noted that, considering that DFIG WTs contain gearboxes, which are known to be the weakest point in the mechanical system, and more likely to be damaged by torque fluctuations than the couplings used in PMSG WTs [25], the $Q_{T(i)}$ is set to 3 for DFIGs, and to 1 for PMSGs.

A. Normal Response of De-loading

In this case, we assume that all turbines are operating under different time-varying wind speeds, as shown in Fig. 3. We further assume that all turbines are initially operating in MPPT mode or at its maximum power limit when, after 20 seconds, the grid operator gives the de-loading signal and the total power output of the WF is suddenly limited to 7.6 MW until 60 s. Then the reference signal keeps continuously changing until the end of the simulation.

Results are shown in Fig. 4. In particular, we compare the results of the decentralized solution with those of a centralized one, to show that despite in the decentralized case the WTs do not communicate any local information, still the same result of the centralized solution is obtained. Accordingly, Fig. 4.(a) shows that the overall power generated by the WF closely follows the desired reference signal, and due to stochastic effects the decentralized solution is only slightly slower than the centralized one, when abrupt changes in the reference signal occur. Fig. 4.(b) shows the generated power of three WTs for easiness of exposition (namely, WT 1, 7 and 10), and

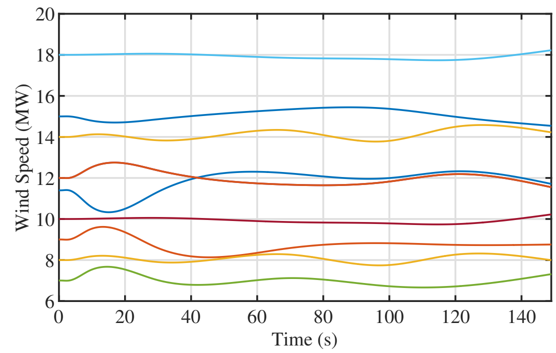

Fig. 3. Varying wind speed experienced by the ten different WTs.

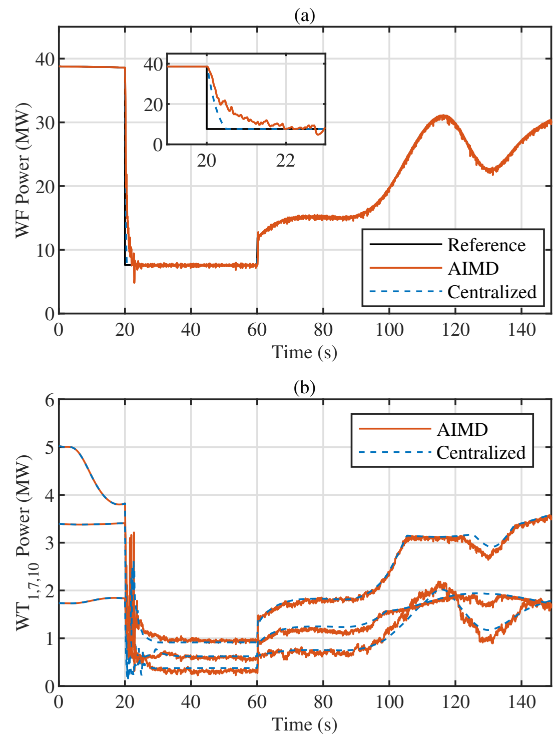

Fig. 4. Power generation of the WF in (a), and power generation of single WTs 1, 7 and 10 in (b).

again the proposed strategy is very similar to the centralized one.

Fig. (5-7) emphasizes the outcome of the optimization problem. The color from blue to red in Fig. 5 corresponds to different utilization hours for each WT. As can be seen, the output results of the proposed decentralized strategy at steady-state satisfy the design purpose, as the outcome is very close to that of the centralized strategy and the newer WTs (i.e., with lower utilization hours) generate on average more power. Finally, the transient behavior of the proposed control methodology is presented in Fig. (6-7). In particular, Fig. 6 shows the evolution of the torque in the two transients, due to the sudden power jump at 20 s and 60 s. While in both cases significant fluctuations are experienced, and despite WT 4 (PMSG) and WT 9 (DFIG) have the same per-unit parameters except different $Q_{T(i)}$ (due to the aforementioned differences in the robustness of the drive mechanisms), the proposed utility

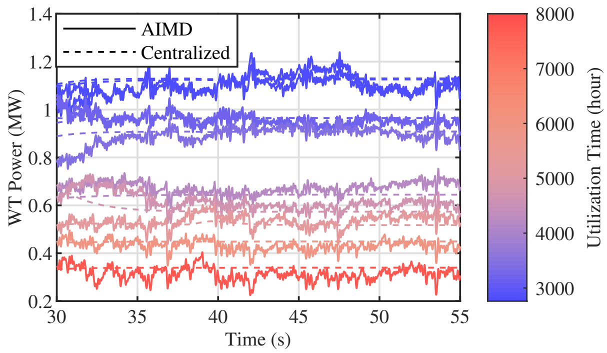

Fig. 5. Power generation of single WTs at steady-state.

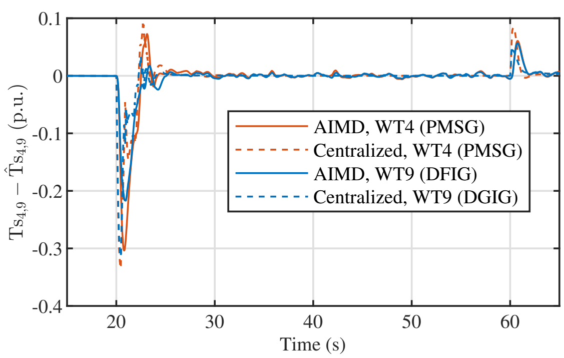

Fig. 6. Torque T_s fluctuation of WTs 4 and 9 at 20 s and 60 s.

functions manage to mitigate the fluctuations of the shaft torque in DFIG WTs, with respect to the PMSG WTs, to reduce possible damages on their weak gearbox. Compared with the centralized solution, the reason why the fluctuation amplitudes of the decentralized method are smaller is that the decentralized method has a slower response speed, which reduces the transient impact to the shaft. Rotor over-speed is most likely to occur when a wind farm sudden drops the output reference (i.e. at 20 s). In Fig. 7, the rotor speed response (based on synchro-speed) of WT 1 for different choices of the weight Q_ω is presented. The outcome shows that when Q_ω is set to zero, then the rotor speed item in the utility function (8) has no effect, and the rotor speed exceeds by 1.32 times the synchro-speed during the transient, which is a common setting value for WT rotor speed protection [26], [27]. This is in practice what may happen when the rotor speed is not taken into account in the utility function, as is common practice. As a contrast, the proposed control with $Q_\omega = 40$ successfully limits the speed below protection settings, just as the centralized solution.

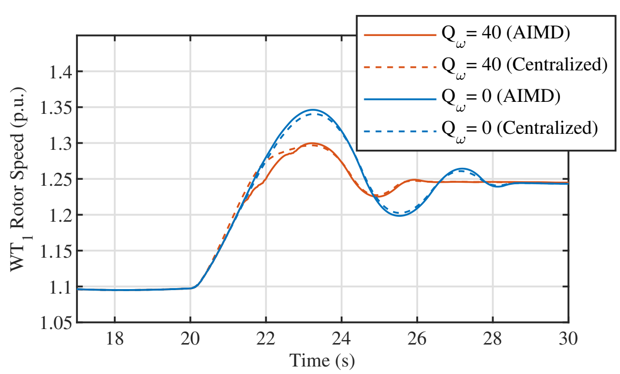

Fig. 7. Rotor speed fluctuation of WT 1 after sudden power droop at 20 s, under different values of the weighting parameter Q_ω .

B. Comparison with Other Power Sharing Techniques

To further demonstrate the effect of the optimization problem, Table II compares the results that are obtained by using our proposed utility function with those that are obtained using the decentralized "fair" strategy (5) [20]. The first two columns give the maximum rotor speed of WTs, which further show that the rotor speeds of the WTs with the proposed method reach smaller values during the transient, and WT 1 with the "fair" strategy also suffers from over-speed problems. Finally, to further evaluate the thrust and torque oscillations, we calculate the mean-square error (MSE) of $\mathrm{d}F_t/\mathrm{d}t$, that penalizes fluctuations of the thrust force, and $|T_s - \hat{T}_s|$, that penalizes deviations from the steady-state torque, in the time interval between 15 and 40 s, which includes the most significant changes of the power reference. The results show that most of the WTs are characterized by mitigated oscillations, when the proposed utility function is considered, with respect to the "fair" strategy.

TABLE II
MAXIMUM ROTOR SPEED, MSE OF $\mathrm{d}F_t/\mathrm{d}t$ AND $|T_s - \hat{T}_s|$, 15 S – 40 S

	Maximum ω_r, (p.u.)		MSE $\mathrm{d}F_t/\mathrm{d}t$, (p.u.)		MSE $\lvert T_s - \hat{T}_s\rvert$, (p.u.)	
	Eq. (8)	Fair	Eq. (8)	Fair	Eq. (8)	Fair
WT1	1.299	1.327	$3.98 \cdot 10^{-4}$	$1.36 \cdot 10^{-3}$	$9.01 \cdot 10^{-3}$	$9.41 \cdot 10^{-3}$
WT2	1.245	1.273	$1.20 \cdot 10^{-4}$	$3.27 \cdot 10^{-4}$	$5.63 \cdot 10^{-3}$	$6.37 \cdot 10^{-3}$
WT3	1.245	1.261	$2.24 \cdot 10^{-4}$	$1.54 \cdot 10^{-3}$	$1.28 \cdot 10^{-2}$	$1.39 \cdot 10^{-2}$
WT4	1.270	1.289	$3.10 \cdot 10^{-4}$	$1.90 \cdot 10^{-3}$	$1.29 \cdot 10^{-2}$	$1.41 \cdot 10^{-2}$
WT5	1.222	1.229	$1.22 \cdot 10^{-5}$	$6.68 \cdot 10^{-7}$	$2.01 \cdot 10^{-3}$	$2.44 \cdot 10^{-3}$
WT6	1.217	1.238	$6.02 \cdot 10^{-5}$	$9.92 \cdot 10^{-4}$	$1.16 \cdot 10^{-2}$	$1.46 \cdot 10^{-2}$
WT7	1.270	1.305	$2.52 \cdot 10^{-4}$	$1.04 \cdot 10^{-3}$	$6.51 \cdot 10^{-3}$	$7.96 \cdot 10^{-3}$
WT8	1.222	1.253	$8.06 \cdot 10^{-5}$	$1.37 \cdot 10^{-3}$	$1.13 \cdot 10^{-2}$	$1.40 \cdot 10^{-2}$
WT9	1.239	1.289	$1.23 \cdot 10^{-4}$	$1.90 \cdot 10^{-3}$	$1.15 \cdot 10^{-2}$	$1.41 \cdot 10^{-2}$
WT10	1.230	1.242	$5.11 \cdot 10^{-5}$	$1.84 \cdot 10^{-6}$	$2.70 \cdot 10^{-3}$	$3.33 \cdot 10^{-3}$

As a further comparison, we now try to evaluate the advantages of our decentralized strategy over distributed ones. The main advantage is that, independently from the choice of a specific utility function, the WTs are not required to communicate any information to either the WF central supervisory agent, or to other WTs. In addition to this, fewer communications are required in general as well. For instance, assuming a step-size of 5 ms, then our MD signal is triggered on average 7.3 times per second, which corresponds to a communication burden of 10 (number of WTs) $\cdot\, 1 \cdot 7.3 = 73$ bits on average. We now evaluate the computational burden of other methodologies, namely, [14]–[17], and we shall consider exactly the same case study with 10 turbines in Table III, but a control frequency of 2 Hz. The results show that although AIMD requires a shorter time-step, our proposed decentralized method greatly reduces the need for communication, whether compared with the centralized control method or the existing distributed strategy.

TABLE III
COMMUNICATION COST PER SECOND*

	AIMD	Centralized	Strategy [14]	Strategy [15]	Strategy [16]	Strategy [17]
Number of targets	5	5	4	2	2	5
Traffic bit per second	73	3,840	7,680	2,368	1,280	5,824

* Assumptions for the assessment are given in Appendix C.

C. Robustness Property of Decentralized Control

One of the most relevant features of the proposed decentralized algorithm is that it is inherently robust against possible failures, as we shall now show in this subsection.

1) "Plug & Play" Features: To demonstrate the "plug & play" features, we assume that the total output of the WF is limited to 22.8 MW and one WT suddenly stops generating power (e.g., due to protection tripping) after 19 s. In this case, no additional communication of such an event is required, and the remaining WTs automatically increase their power generation, proportionally to their utility functions, as shown in Fig. 8.(a), so that the overall generated power keeps matching the reference signal, as shown in Fig. 8.(b). Obviously, a similar behaviour is observed if one WT suddenly starts generating power (e.g., because it has finished undergoing maintenance operations).

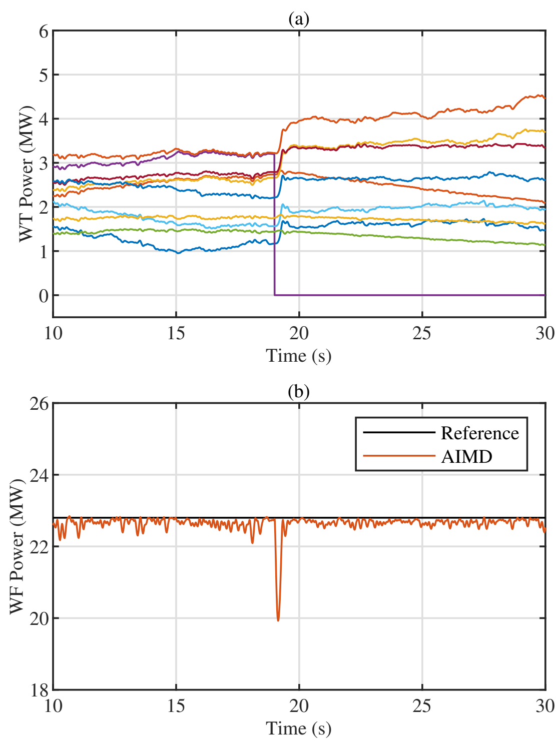

Fig. 8. After 19 seconds one WT stops providing power, and all the other WTs automatically increase their share of generated power, as shown in (a). At all times, the overall power generated by the WF seamlessly matches the desired one (b).

2) Link Failures: Here we simulate what happens if one of the ten WTs' communication lines is disconnected after 19 s. Roughly speaking, since this WT does not receive any back-off signal anymore by the WF, it will start generating as much power as possible, and the other WTs adjust their power generation so that the overall matching goal is still achieved, as shown in Fig. 9. So, the main goal of the WF is still satisfied.

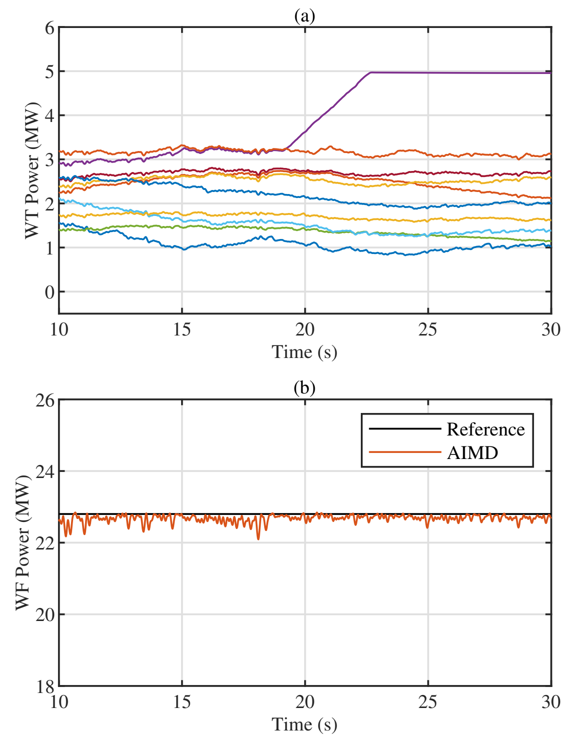

Fig. 9. After 19 seconds the communication line of one WT suddenly disconnected. The corresponding WT incrementally increases its output until the rated power, as shown in (a). At all times, the overall power generated by the WF seamlessly matches the desired one (b).

3) Random Packet Losses: We now investigate what happens if some signals sent by the supervisory controller are randomly lost. For this purpose, we assume that each WT has a 50% probability of either receiving, or failing to receive, the Multiplicative Decrease (MD) signal. We can observe from Fig. 10 that convergence is slower than when all signals are correctly received, but still, the total output still meets the power reference of the wind farm (and power generation is optimally shared among the WTs).

It is important to note that for the above three examples with unexpected failures, this automatic redistribution of power generation occurs without any further communication required with respect to the nominal operation.

V. CONCLUSIONS

An AIMD-based decentralized methodology sharing the power in de-loading operations of WTs in a WF was proposed and validated in the paper. In particular, the power was

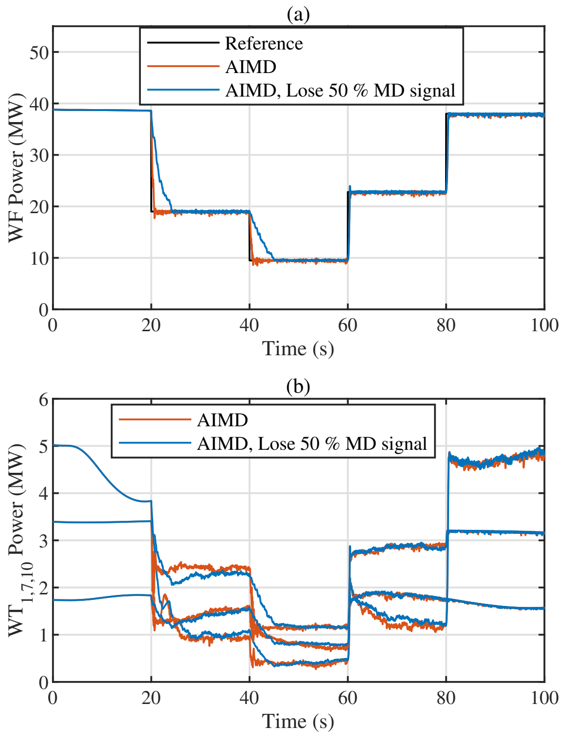

Fig. 10. 50% of the MD signals sent by the supervisory controller to the WTs randomly fail, the total output still meets the power reference of a wind farm, as shown in (a). At all times, the overall power generated by the WF seamlessly matches the desired one (b).

shared according to utility functions that take into account individual mechanical and rotor speed stresses during the de-loading transient, and prioritize the utilization of newer turbines near their optimal working point to eventually balance the aging of WTs in a WF. The method is very attractive and efficient for practical applications, as optimal power sharing is obtained in a fully decentralized fashion, without requiring complex communication networks or frequent bidirectional communications, even when unexpected failures locally occur. Another interesting feature of AIMD algorithms is that not all WTs need to have the same utility functions and parameters, which allows one to consider different ages or different manufacturers. Simulation results confirm the effectiveness of the proposed wind farm controller in optimizing reference power for VSWT in a way that fluctuations of tower torque, thrust and generator speed decrease significantly, and generation from newer WTs is prioritized at steady-state. The matching between the power requested by the outer grid and that generated by the wind farm is shown to occur also under different faulty conditions.

Appendix A
Practical Computation of the Utility Function

In order to successfully implement our proposed decentralized control, each WT i needs to find out how its power reference $P_{ref(i)}$ influences the corresponding $f_i(\cdot)$ by local measurements and computations. Obviously, the steady-state component (the last part in (8)) only depends on the value of $P_{ref(i)}$. Hence the rest of this subsection focuses on how to calculate the transient part (the first three components of the utility function (8)).

The procedure to compute the first two components of the utility function can be found in classic references [10], [14], [17], and here we briefly recall it for convenience. The basic idea is to adopt a state-space model, obtained through a linearization procedure around the operating point, rather than the complicated actual non-linear VSWT mechanical rotation model described in Section II-A.

More specifically, a VSWT (1), (2), (4) with pitch controller (Figure 1) can be approximately represented by an incremental state-space model:

$$\begin{aligned} \dot{x} &= \boldsymbol{A}x + \boldsymbol{B}u + \boldsymbol{E} \\ y &= \boldsymbol{C}x + \boldsymbol{D}u \end{aligned} \tag{11}$$

where

$$x = \begin{bmatrix} \theta \\ \omega_r \\ \omega_f \end{bmatrix}, y = \begin{bmatrix} T_s \\ F_t \end{bmatrix}, u = \begin{bmatrix} P_{ref(i)} \end{bmatrix}. \tag{12}$$

The coefficient matrices $\boldsymbol{A}$, $\boldsymbol{B}$, $\boldsymbol{E}$ in the state equations are given as follows, where the subscript "0" refers to the linearization around the operating point

Case 1: Constant pitch angle

$$\begin{aligned} \boldsymbol{A} &= \begin{bmatrix} 0 & 0 & 0 \\ \frac{1}{J_t}\frac{\partial T_r}{\partial \theta} & \frac{1}{J_t}(\frac{\partial T_r}{\partial \omega_r} + \frac{P_{ref0}}{\omega_{r0}^2}) & 0 \\ 0 & \frac{1}{\tau_f} & -\frac{1}{\tau_f} \end{bmatrix}, \\ \boldsymbol{B} &= \begin{bmatrix} 0 \\ \frac{P_{ref0}}{\omega_{r0}^2} \\ 0 \end{bmatrix}, \ \boldsymbol{E} = \begin{bmatrix} 0 \\ \frac{1}{J_t}(T_{r0} - T_{e0}) \\ 0 \end{bmatrix}. \end{aligned} \tag{13}$$

Case 2: Pitch angle control when $|\mathrm{d}\theta_{PI}/\mathrm{d}t| \leq \dot{\theta}_{max}$ ($\boldsymbol{B}$ is the same as in Case 1)

$$\begin{aligned} \boldsymbol{A} &= \begin{bmatrix} 0 & \frac{K_p}{\tau_f} & K_i - \frac{K_p}{\tau_f} \\ \frac{1}{J_t}\frac{\partial T_r}{\partial \theta} & \frac{1}{J_t}(\frac{\partial T_r}{\partial \omega_r} + \frac{P_{ref0}}{\omega_{r0}^2}) & 0 \\ 0 & \frac{1}{\tau_f} & -\frac{1}{\tau_f} \end{bmatrix}, \\ \boldsymbol{E} &= \begin{bmatrix} K_i(\omega_{f0} - \omega_n) \\ \frac{1}{J_t}(T_{r0} - T_{e0}) \\ 0 \end{bmatrix}. \end{aligned} \tag{14}$$

Case 3: Pitch angle control when $|\mathrm{d}\theta_{PI}/\mathrm{d}t| > \dot{\theta}_{max}$ ($\boldsymbol{A}$, $\boldsymbol{B}$ are the same as in Case 1)

$$\boldsymbol{E} = \begin{bmatrix} \pm\dot{\theta}_{max} \\ \frac{1}{J_t}(T_{r0} - T_{e0}) \\ 0 \end{bmatrix}. \tag{15}$$

The coefficient matrices $\boldsymbol{C}$, $\boldsymbol{D}$ in output-equation are:

$$\boldsymbol{C} = \begin{bmatrix} \frac{J_g}{J_t}\frac{\partial T_r}{\partial \theta} & -\frac{J_r}{J_t}\frac{P_{ref0}}{\omega_{r0}^2} + \frac{J_g}{J_t}\frac{\partial T_r}{\partial \omega_r} & 0 \\ \frac{\partial F_t}{\partial \theta} & \frac{\partial F_t}{\partial \omega_r} & 0 \end{bmatrix}, \boldsymbol{D} = \begin{bmatrix} \frac{J_r}{J_t \omega_{r0}} \\ 0 \end{bmatrix}. \tag{16}$$

The discretized model of the state-space representation (11) can be states as follows:

$$\begin{aligned} x(t + \Delta\tau_s) &= \boldsymbol{A}_d x(t) + \boldsymbol{B}_d u(t) + \boldsymbol{E}_d \\ y(t) &= \boldsymbol{C}_d x(t) + \boldsymbol{D}_d u(t) \end{aligned} \tag{17}$$

where $\Delta\tau_s$ is the sampling time, and

$$x(t) = \begin{bmatrix} \theta(t) \\ \omega_r(t) \\ \omega_f(t) \end{bmatrix}, y(t) = \begin{bmatrix} T_s(t) \\ F_t(t) \end{bmatrix}, u(t) = \begin{bmatrix} P_{ref(i)}(t) \end{bmatrix}. \quad (18)$$

If we reasonably assume that the input $P_{ref(i)}(t)$ remains constant during the sample interval $\Delta\tau_s$, then the output of the next time step can be obtained as:

$$y(t+\Delta\tau_s) = \boldsymbol{C}_d x(t+\Delta\tau_s) + \boldsymbol{D}_d u(t). \quad (19)$$

In the first term of the utility function, there appears the quantity $\mathrm{d}F_t/\mathrm{d}t$, and following the discussion in [10], [14], [17], it can be estimated by using the discretized models (17), (19) and the input $P_{ref(i)}(t)$, as follows:

$$\frac{\mathrm{d}F_t}{\mathrm{d}t} = \frac{F_t(t+\Delta\tau_s) - F_t(t)}{\Delta\tau_s}. \quad (20)$$

In the second term of the utility function, T_s is the shaft torque as usual and it corresponds to the first output of model (11), and thus it can be computed as a linear combination of the measured states and the input $P_{ref(i)}$. In addition, $\hat{T}_s$ denotes its average value, and it can be obtained by filtering T_s through a low-pass filter.

In the third term of the utility function, one should be aware that when VSWTs reach the maximum predicted rotor speed ω_{pre} in (9) the system may be far from the nominal operating point, and the linearized model (11) [10], [14], [17] may not be an accurate approximation anymore. Accordingly, time-domain numerical integration methods are usually adopted as an alternative. As the speed typically fluctuates with a relatively large time constant and reaches its maximum within a few seconds, as from the rotor motion equations (1) and (2), then the time domain integration step does not have to be too small (and this is convenient for reducing the computational time).

APPENDIX B

The parameters of WTs are presented in Table IV, where note that the generator inertia of DFIG-based WTs is expressed in terms of the low-speed shaft. In addition, the utilization hours of WTs are given in Table V.

APPENDIX C

It is assumed that the centralized and distributed control strategies [14]–[17] are also implemented in a wind farm with 10 WTs. The communication network adopts the simplest topology for each strategy without any redundancy. All slowly transferred data are ignored (for instance, the maximum generating capacity of WTs in [14] and utilization hours in our proposed method). The variables transferred are 32-bit floating-point data with a refresh rate of 2 Hz. The "targets" field refers to the number of controlled quantities (i.e., the wind farm output, plus other terms appearing in the utility function). Generally speaking, more targets require more data to be collected and transmitted.

TABLE IV
PARAMETERS OF WIND TURBINE MODEL

Symbol	Description	Value
v_{wn}	Rated wind speed $[\mathrm{m/s}]$	11.4
R	Rotor radius $[\mathrm{m}]$	63
J_R	Rotor inertia $[\mathrm{kg\cdot m^2}]$	11,776,047
ω_n	Rotor rate speed $[\mathrm{rpm}]$	12.1
η	Gearbox ratio (only for DFIG)	97
J_G	Generator inertia $[\mathrm{kg\cdot m^2}]$	5,025,497
ω_n/ω_s	Rated rotor speed / synchronous speed	1.2
ρ	Air density $[\mathrm{kg/m^3}]$	1.225
K_p	Proportional gain of the pitch control	200
K_i	Integral gain of the pitch control	5
$\dot{\theta}_{max}$	Maximum pitch regulation rate $[\mathrm{deg/s}]$	5
τ_f	Time constant of pitch control low-pass filter $[\mathrm{s}]$	0.1

REFERENCES

[1] S. Chatterjee and S. Chatterjee, "Review on the techno–commercial aspects of wind energy conversion system," IET Renewable Power Generation, vol. 12, pp. 1581–1608, October 2018.
[2] Z. Chen, J.M. Guerrero, and F. Blaabjerg, "A Review of the State of the Art of Power Electronics for Wind Turbines," IEEE Transactions on Power Electronics, vol. 24, pp. 1859–1875, August 2009.
[3] Z. Song, F. Shen, Z. Nan, Y. Zhang, L. Zhao, X. Deng, N. Zhang, H. Li, Z. Zhang, W. Ye, and T. Lu, "Power grid planning based on differential abandoned wind rate," The Journal of Engineering, vol. 2017, pp. 1055–1059, October 2017.
[4] M. Zhou, Z. Dong, H. Li, C. Gan, G. Li, and Y. Liu, "Coordinated Control of DFIG Based Wind Farms and SGs for Improving Transient Stability," IEEE Access, vol. 6, pp. 46844–46855, September 2018.
[5] S. Wang and K. Tomsovic, "A Novel Active Power Control Framework for Wind Turbine Generators to Improve Frequency Response," IEEE Transactions on Power Systems, vol. 33, pp. 6579–6589, November 2018.
[6] T. Surinkaew and I. Ngamroo, "Hierarchical Co-Ordinated Wide Area and Local Controls of DFIG Wind Turbine and PSS for Robust Power Oscillation Damping," IEEE Transactions on Sustainable Energy, vol. 7, pp. 943–955, July 2016.
[7] P. Flores, A. Tapia, and G. Tapia, "Application of a control algorithm for wind speed prediction and active power generation," Renewable Energy, vol. 30, pp. 523–536, April 2005.
[8] R.G. De Almeida, E.D. Castronuovo, and J.A. Pecas Lopes, "Optimum Generation Control in Wind Parks When Carrying Out System Operator Requests," IEEE Transactions on Power Systems, vol. 21, pp. 718–725, May 2006.
[9] A.D. Hansen, P. Sørensen, F. Iov, and F. Blaabjerg, "Centralised power control of wind farm with doubly fed induction generators," Renewable Energy, vol. 31, pp. 935–951, June 2006.
[10] V. Spudić , M. Jelavić, and M. Baotić. "Wind Turbine Power References in Coordinated Control of Wind Farms,"Automatika, vol.52, pp. 82–94, February 2011.
[11] Y. Li, Z. Xu, and K. Meng, "Optimal Power Sharing Control of Wind Turbines," IEEE Transactions on Power Systems, vol. 32, pp. 824–825, April 2017.
[12] X. Lyu, Y. Jia, and Z. Xu, "A Novel Control Strategy for Wind Farm Active Power Regulation Considering Wake Interaction," IEEE Transactions on Sustainable Energy, in press.
[13] F.M. Ebrahimi, A. Khayatiyan, and E. Farjah, "A novel optimizing power control strategy for centralized wind farm control system," Renewable Energy, vol. 86, pp. 399-408, February 2016.
[14] H. Zhao, Q. Wu, Q. Guo, H. Sun, and Y. Xue, "Distributed Model Predictive Control of a Wind Farm for Optimal Active Power Control, Part II: Implementation With Clustering-Based Piece-Wise Affine Wind Turbine Model," IEEE Transactions on Sustainable Energy, vol. 6, pp. 840–849, July 2015.
[15] S. Baros and M.D. Ilic, "Distributed Torque Control of Deloaded Wind DFIGs for Wind Farm Power Output Regulation," IEEE Transactions on Power Systems, vol. 32, pp. 4590–4599, November 2017.
[16] J. Zhang, Y. Li, Z. Xu, D. Qi, and C. Li, "Game theory-based optimal deloading control of wind turbines under scalable structures of wind farm," IET Cyber-Physical Systems: Theory & Applications, 3, pp. 224-231, December 2018.

TABLE V
UTILIZATION HOURS OF WTs

WT No.	1	2	3	4	5	6	7	8	9	10
Utilization Hours $t_{u(i)}$	7,865	3,247	3,461	2,760	5,260	6,025	3,247	4,253	2,760	4,760

[17] Y. Guo, H. Gao, Q. Wu, J. Østergaard, D. Yu, and M. Shahidehpour, ”Distributed coordinated active and reactive power control of wind farms based on model predictive control,” International Journal of Electrical Power & Energy Systems, vol. 104, pp. 78–88, January 2019.
[18] D. Chiu and R. Jain, “Analysis of the Increase/Decrease Algorithm for Congestion Avoidance in Computer Networks,” Journal of Computer Networks, vol. 17, pp. 1–14, June 1989.
[19] M. Corless, C. King, R. Shorten, and F. Wirth, AIMD Dynamics and Distributed Resource Allocation. Philadelphia, PA, USA: SIAM, 2016.
[20] X. Fan, E. Crisostomi, D. Thomopulos, B. Zhang, and R. Shorten, “A Decentralized Power Sharing Strategy for Wind Farm De-Loading,” accepted by the IEEE Power and Energy Society General Meeting (GM PES), 2020. [Online]. Available: https://www.dropbox.com/s/79qov179j8372z4/conference.pdf?dl=0
[21] J. Jonkman and S. Butterfield and W. Musial, and G. Scott, “Definition of a 5-MW Reference Wind Turbine for Offshore System Development,” National Renewable Energy Laboratory, US, 2009. [Online]. Available: http://www.nrel.gov/wind/pdfs/38060.pdf
[22] Walford, C. A., “Wind turbine reliability: understanding and minimizing wind turbine operation and maintenance costs,” Sandia National Laboratories, No. SAND2006-1100, March 2006.
[23] W. Griggs, J. Y. Yu, F. Wirth, F. Häuesler, and R. Shorten “On the design of campus parking systems with QoS guarantees,” IEEE Transactions on Intelligent Transportation Systems, vol. 17, pp. 1428–1437, May 2016.
[24] F. R. Wirth, S. Stüdli, J. Y. Yu, M. Corless, and R. Shorten, “Nonhomogeneous Place-dependent Markov Chains, Unsynchronised AIMD, and Optimisation,” Journal of the ACM, vol 66, pp. 1–37, August 2019.
[25] W. Dong, Y. Xing, T. Moan, and Z. Gao. “Time domain-based gear contact fatigue analysis of a wind turbine drivetrain under dynamic conditions,” International Journal of Fatigue, vol. 48, pp. 133–146, March 2013.
[26] Xuji, “WT2000 / 93 technical specification,” XJ Group, Xuchang, China, 2010.
[27] Guodian United Power, “UP82-III Wind turbine technical specifications,” Guodian United Power Technology CO., LTD. , Beijing, China, December 2009.

Xinkai Fan received the B.S. degree in electrical engineering from Xi’an Jiaotong University, China, in 2015. He is currently pursuing the Ph.D. degree in the school of Electrical Engineering in Xi’an Jiaotong University, and now is also a visiting student at the University of Pisa. His main field of interest includes the control for renewable energy, HVDC, and power system transient stability analysis.

Emanuele Crisostomi received the B.S. degree in computer science engineering, the M.S. degree in automatic control, and the Ph.D. degree in automatics, robotics, and bioengineering, from the University of Pisa, Italy, in 2002, 2005, and 2009, respectively. Since 2011 he has been with the Department of Energy, Systems, Territory and Constructions Engineering, University of Pisa, first as an assistant professor, and since 2017 as an associate professor of electrical systems. His research interests include control and optimization of large-scale systems, with applications to smart grids and green mobility networks.

Dimitri Thomopulos was born in Bologna, Italy, in 1987. He received the M.Sc. degree in Business and Industrial Engineering and Ph.D. in Automatic Control Systems and Operational Research from the University of Bologna, Bologna, Italy in 2012 and in 2016, respectively. From 2017 to 2018, he was a Post-Doctoral Researcher at LIX CNRS - École Polytechnique, Palaiseau, France. He is currently Research Fellow at the University of Pisa. His current research interests include: combinatorial optimization, non-linear optimization, mostly applied to energy problems; power-systems, micro-grids, hydro unit commitment, and wind farm optimization; computational intelligence and big data analysis, with applications in electromagnetism.

Baohui Zhang was born in Hebei Province, China, in 1953. He received the M.Eng. and Ph.D. degrees in electrical engineering from Xi’an Jiaotong University, Xi’an, China, in 1982 and 1988, respectively. He has been a Professor in the Electrical Engineering Department at Xi’an Jiaotong University since 1992. His research interests are system analysis, control, communication, and protection.

Robert Shorten received the B.E. degree (first-class honors) from the University College Dublin (UCD) in 1990 in electronic engineering. He received the Ph.D. degree in 1996, also from UCD, while based in at Daimler-Benz Research in Berlin, Germany. From 1993 to 1996, he was the holderof a Marie Curie Fellowship at Daimler-Benz Research to conduct research in the area of smart gearbox systems. Following a brief spell at theCenter for Systems Science, Yale University, working with Professor K. S. Narendra, he returned to Ireland as the holder of a European Presidency Fellowship in 1997. He is a co-founder of the Hamilton Institute at NUI Maynooth, where he was a full Professor until March 2013. He was also a Visiting Professor at TU Berlin from 2011–2012. He is currently a Senior Research Manager at IBM Research Ireland. His research spans a number of areas. He has been active in computer networking, automotive research, collaborative mobility (including smart transportation and electric vehicles), as well basic control theory and linear algebra. His mainfield of theoretical research has been the study of hybrid dynamical systems

Songhao Yang was born in Shandong, China, in 1989. He received the B.S. and Ph.D. degrees in electrical engineering from the Xi’an Jiaotong University, Xi’an, China, in 2012 and 2019, respectively. Besides, he received the Ph. D degree in electrical and electronic engineering from Tokushima University, Japan, in 2019. Currently, he is an Assistant Professor at Xi’an Jiaotong University. His research interests are renewable energy penetrated power system stability analysis and control.